Electronic Supplementary Material (ESI) for Inorganic Chemistry Frontiers.

Supporting Information

Photoreforming of polyester plastics into added-value chemicals coupling with H_2 evolution over a $Ni_2P/ZnIn_2S_4$ catalyst

Chu-Xuan Liu,[ab] Rui Shi,[a] Wangjing Ma,[a] Fulai Liu*[a] and Yong Chen *[ab]

[a]Key Laboratory of Photochemical Conversion and Optoelectronic Materials, CAS-HKU Joint Laboratory on New Materials, Technical Institute of Physics and Chemistry, Chinese Academy of Sciences, CAS, Beijing 100190, P.R. China

[b]University of Chinese Academy of Sciences, Beijing 100049, P.R. China

*E-mail: chenyong@mail.ipc.ac.cn; liufulai@mail.ipc.ac.cn

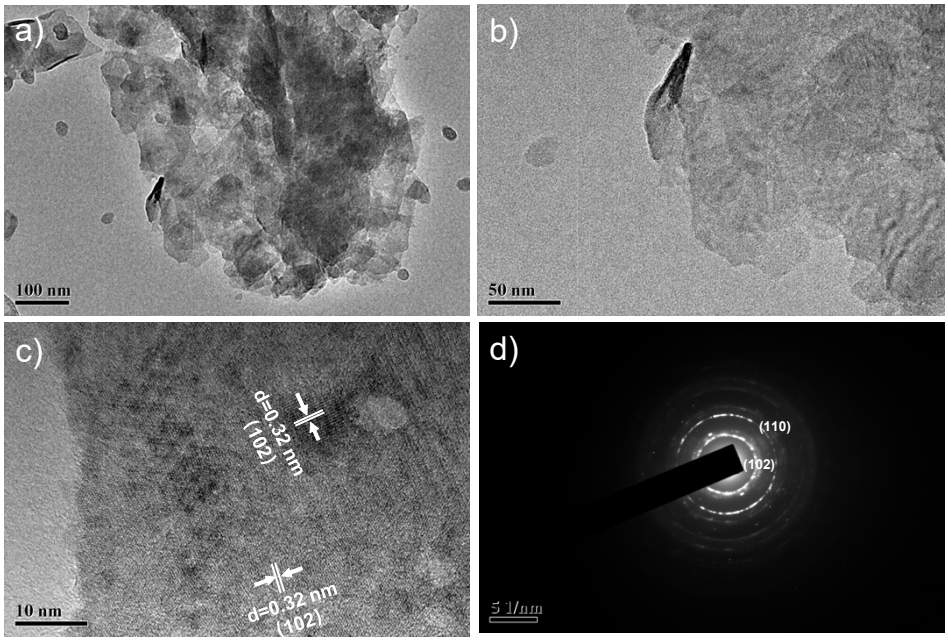

Fig. S1 a-b) TEM and c) high-resolution TEM images of pristine $ZnIn_2S_4$ nanosheets; d) SAED pattern of pristine $ZnIn_2S_4$ nanosheets.

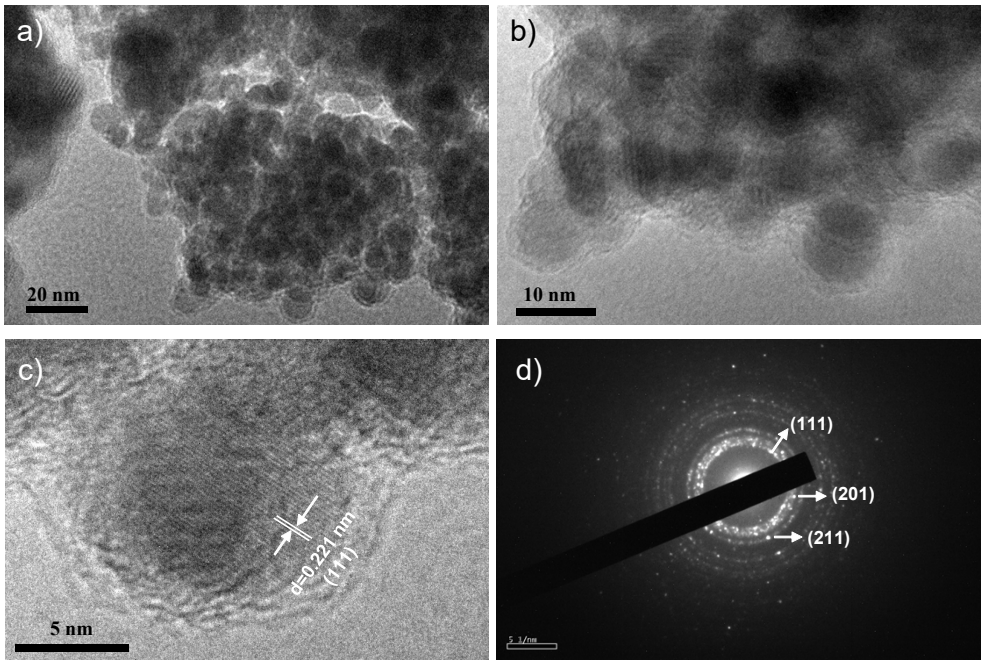

Fig. S2 a-b) TEM and c) high-resolution TEM images of pure Ni_2P nanoparticles; d) SAED pattern of pure Ni_2P nanoparticles.

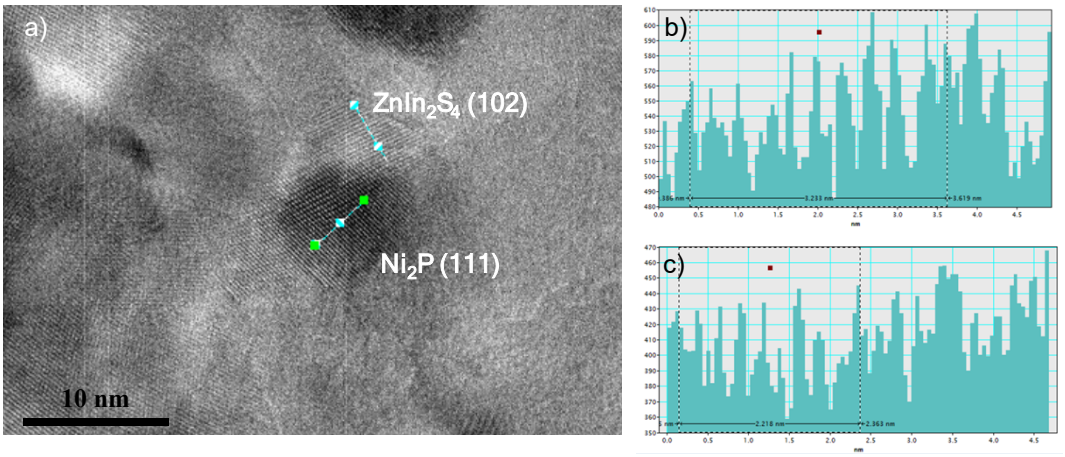

Fig. S3 a) high-resolution TEM image of $Ni_2P/ZnIn_2S_4$; b-c) intensity profile of $ZnIn_2S_4$ and Ni_2P crystal face.

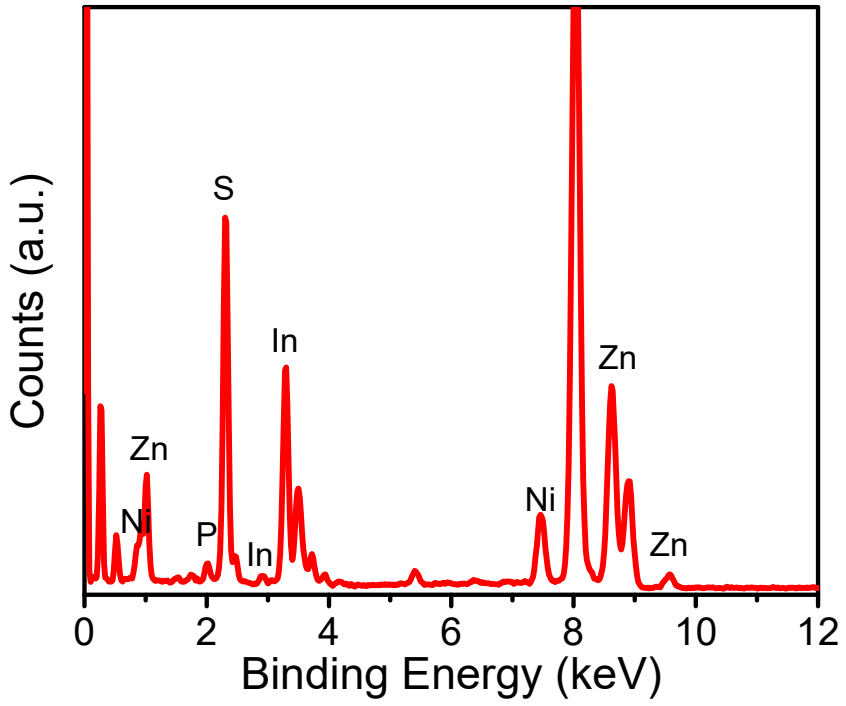

Fig. S4 EDX spectrum of the $Ni_2P/ZnIn_2S_4$ composites.

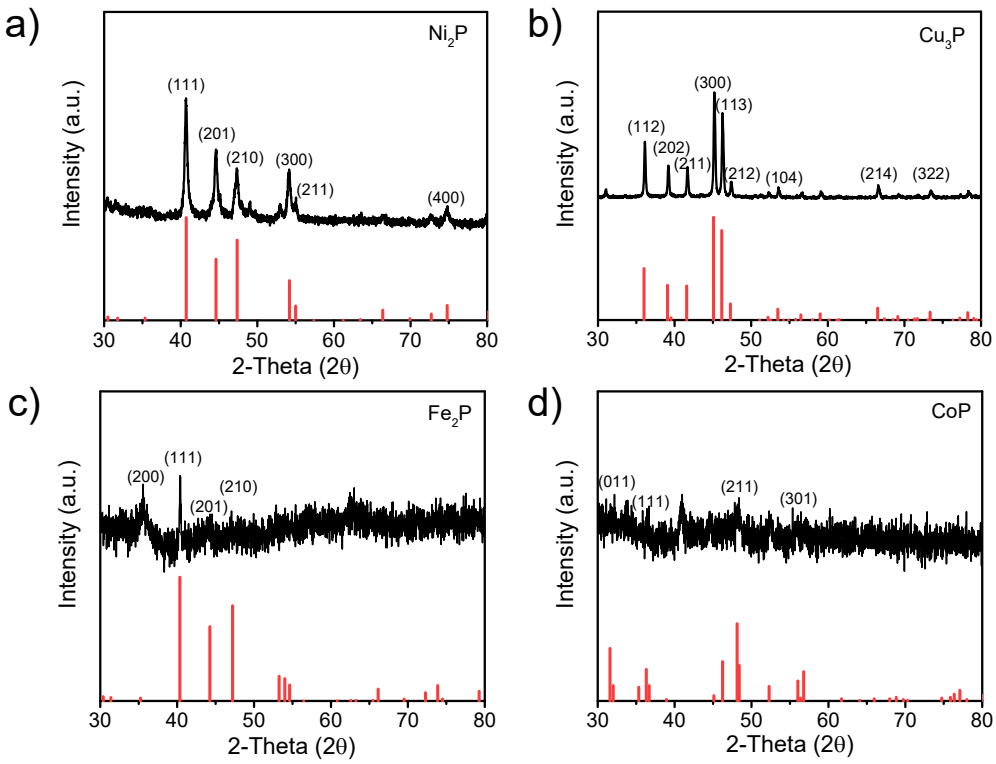

Fig. S5 The XRD patterns of a) Ni_2P; b) Cu_3P; c) Fe_2P; d) CoP samples.

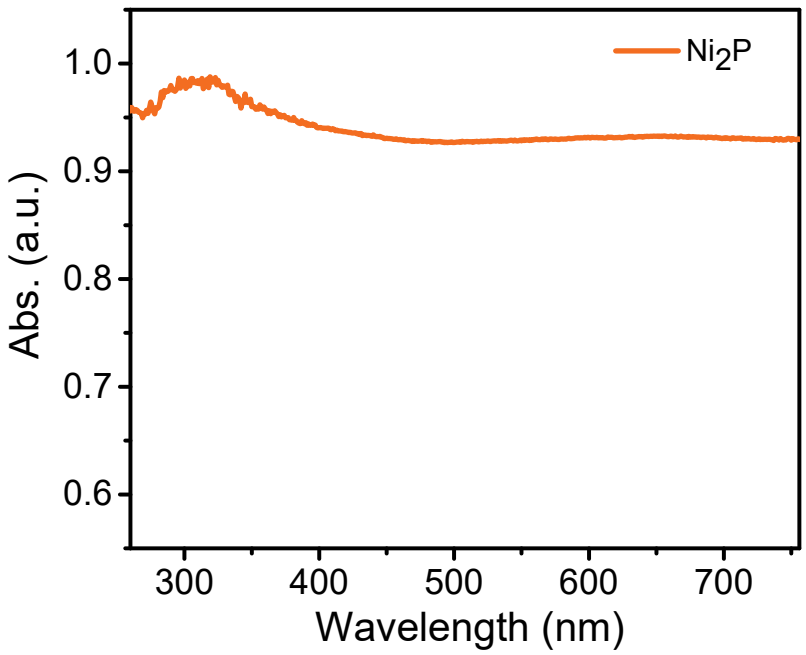

Fig. S6 UV-vis DRS spectrum of Ni_2P nanoparticles.

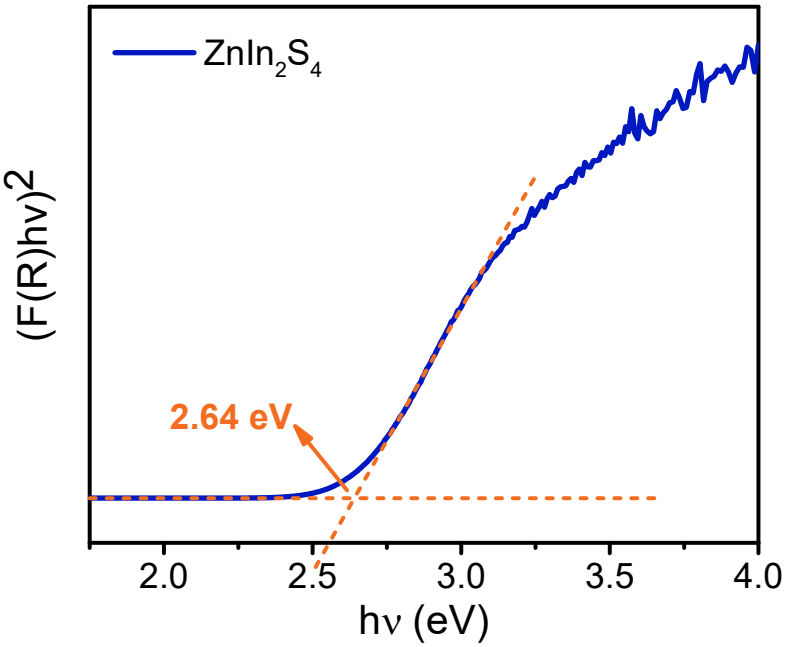

Fig. S7 Curve of $(h\nu)^2$ versus the energy of the exciting light ($h\nu$) of $ZnIn_2S_4$.

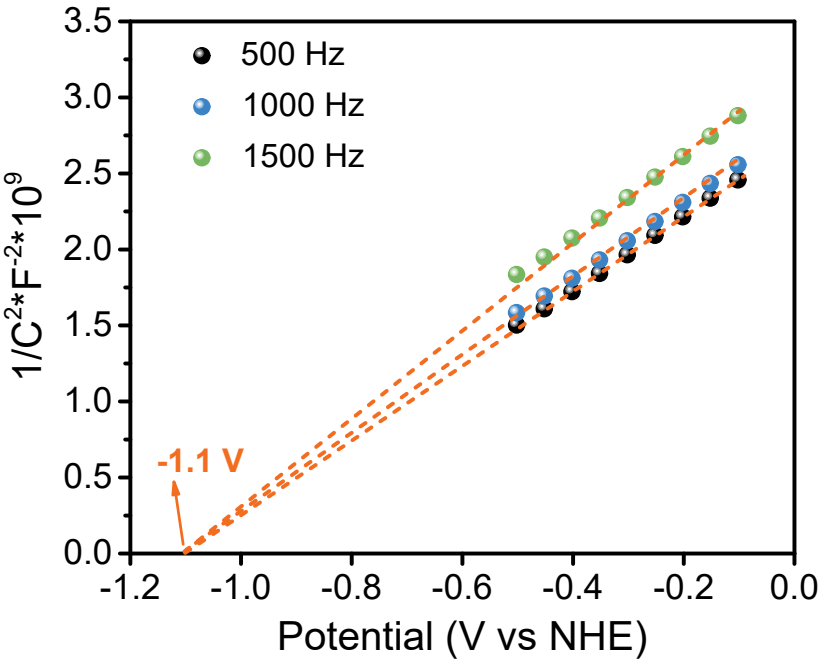

Fig. S8 Mott-Schottky plots of $ZnIn_2S_4$.

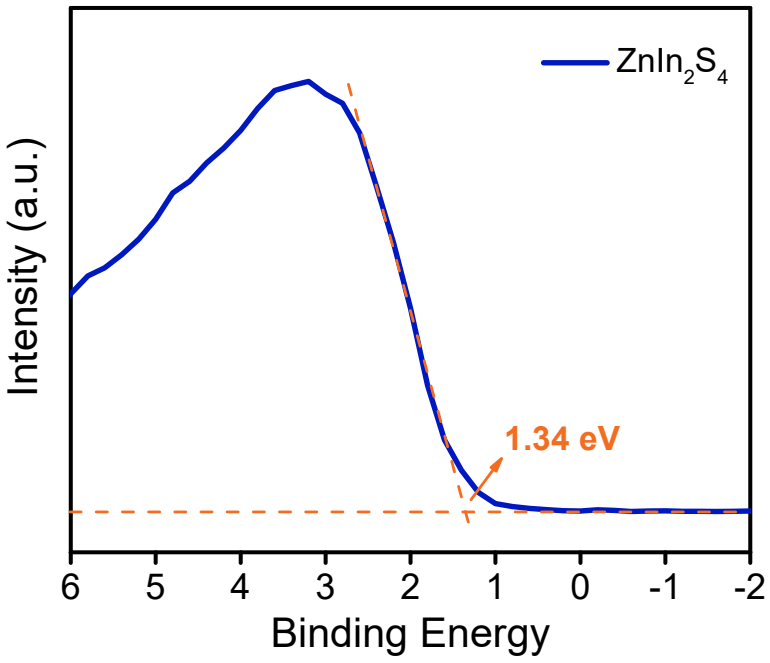

Fig. S9 The valence band spectrum of $ZnIn_2S_4$.

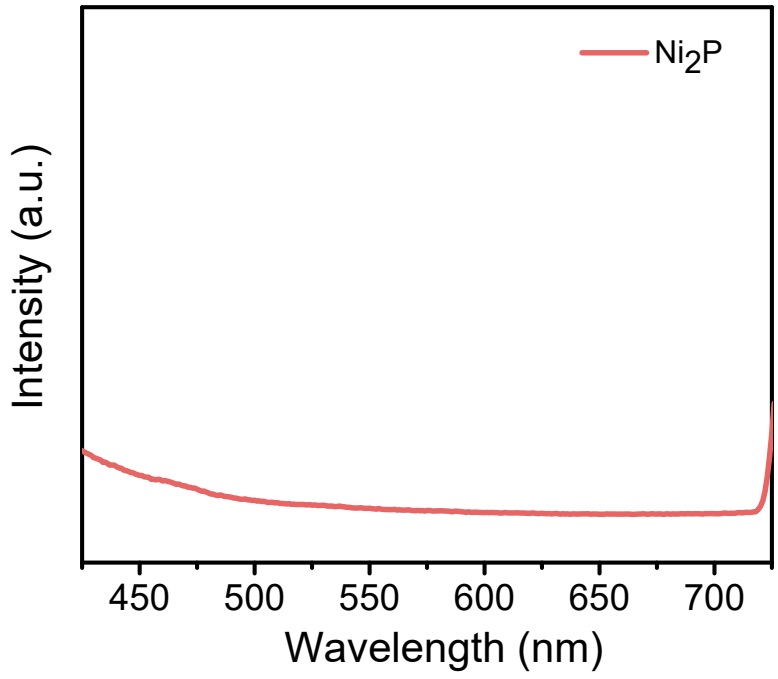

Fig. S10 PL spectrum of Ni_2P nanoparticles.

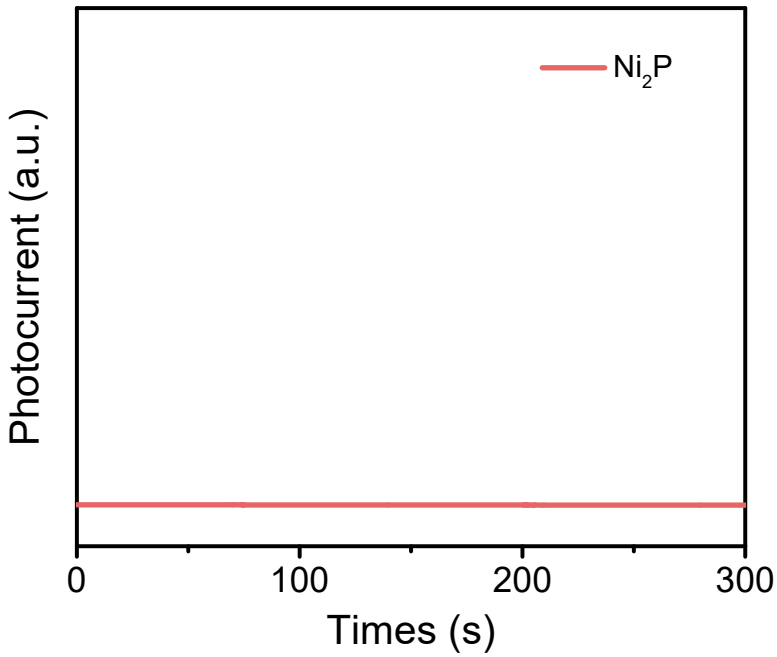

Fig. S11 The photocurrent response of Ni_2P nanoparticles.

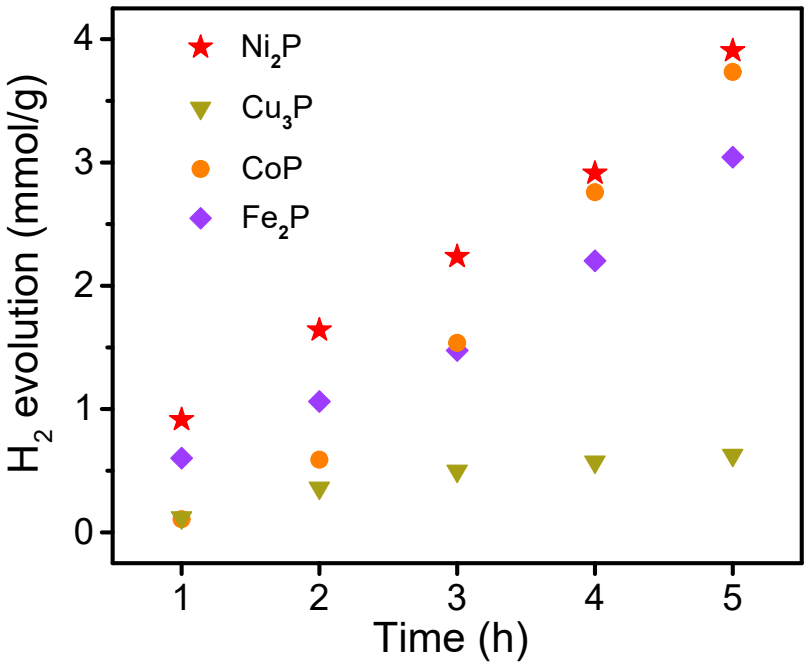

Fig. S12 Time-dependent H_2 evolution plots of $Ni_2P/ZnIn_2S_4$, $CoP/ZnIn_2S_4$, $Fe_2P/ZnIn_2S_4$, $Cu_3P/ZnIn_2S_4$ under visible light irradiation ($\lambda > 420$ nm) in 0.1 M PLA hydrolysate.

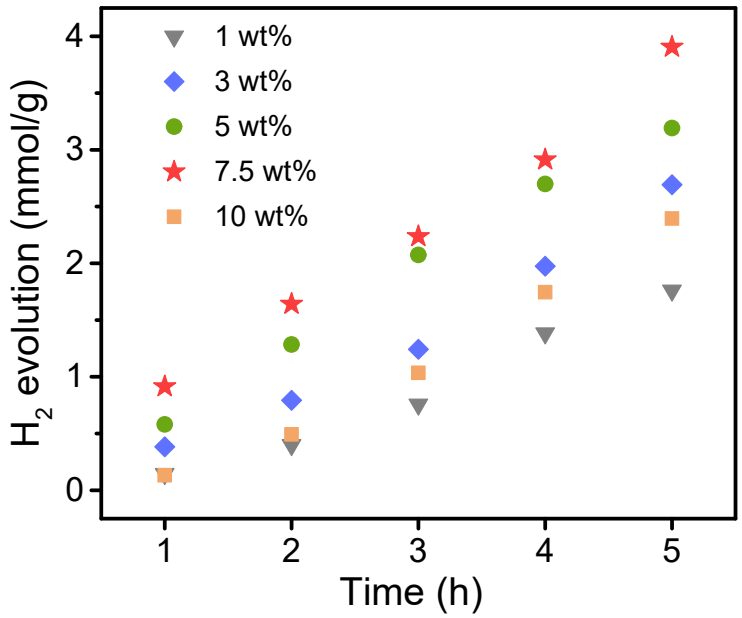

Fig. S13 Time-dependent H_2 evolution plots of $Ni_2P/ZnIn_2S_4$ with different mass ratio under visible light irradiation ($\lambda > 420$ nm) in 0.1 M PLA hydrolysate.

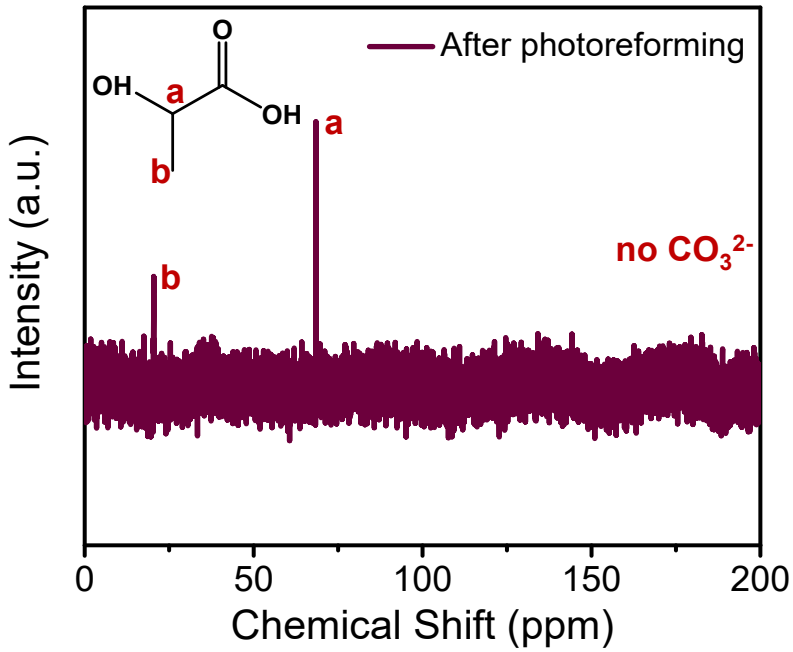

Fig. S14 ^{13}C NMR of pretreated PLA after photoreforming for 24h.

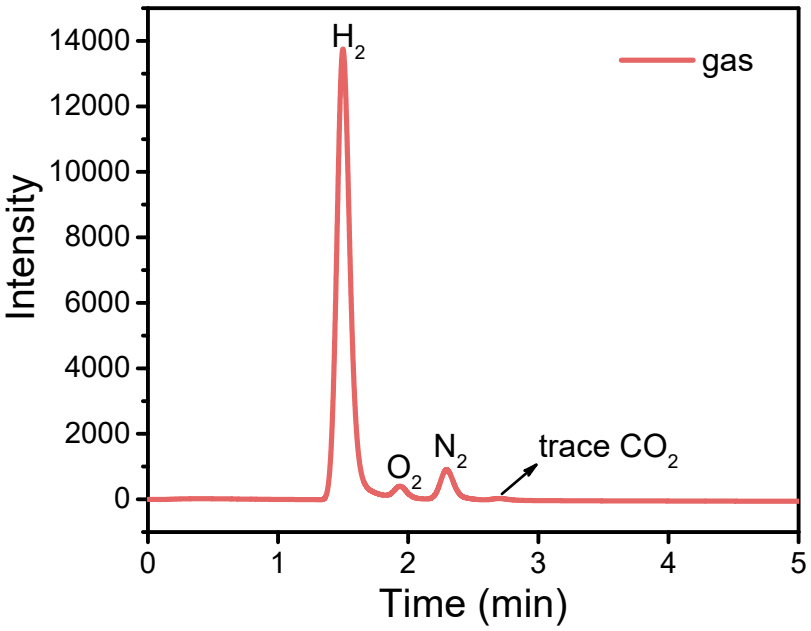

Fig. S15 GC spectrum of the generated gas after photoreforming.

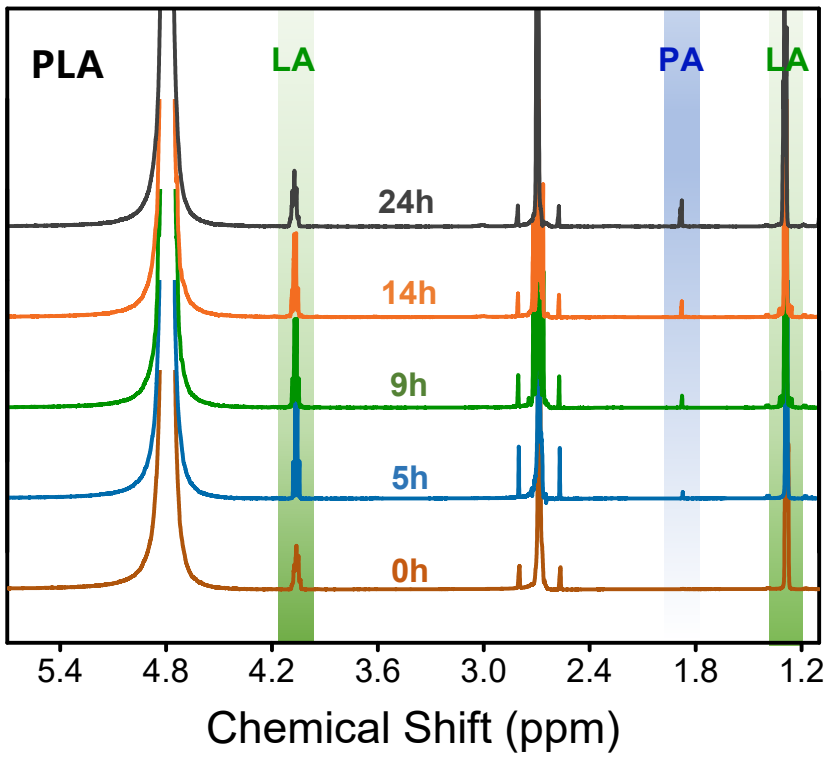

Fig. S16 ^{1}H NMR measurements of PLA oxidation.

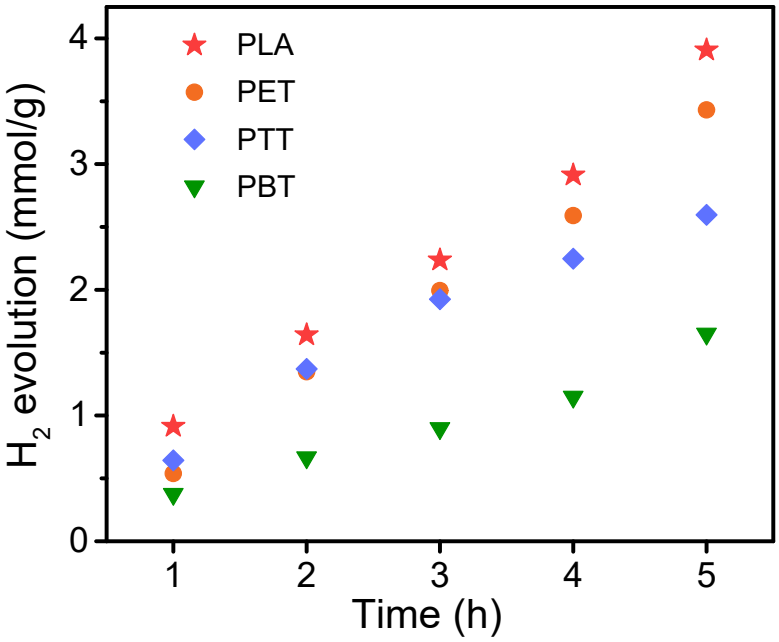

Fig. S17 Time-dependent H_2 evolution plots of 7.5-$Ni_2P/ZnIn_2S_4$ under visible light irradiation ($\lambda > 420$ nm) in 0.1 M different plastic hydrolysates.

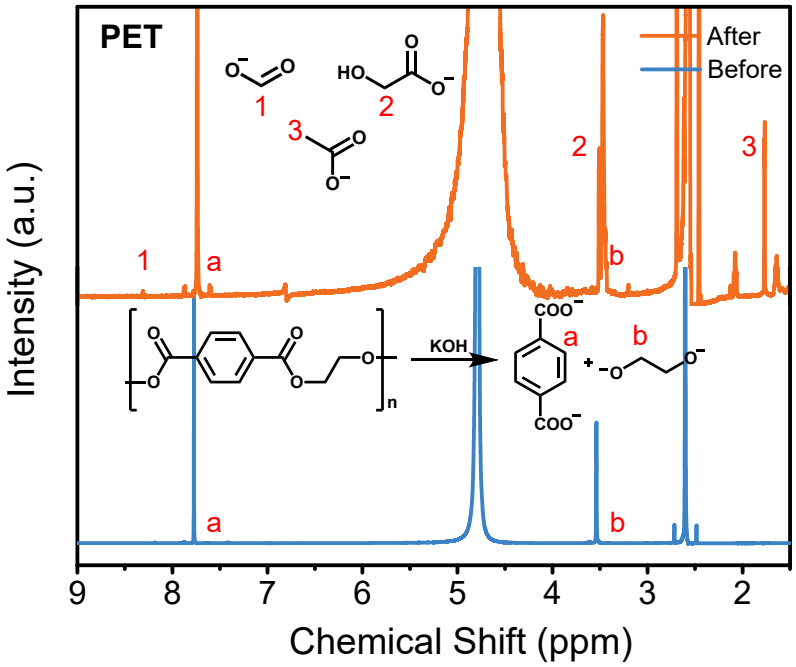

Fig. S18 ^1H NMR spectra of products before and after photoreforming of PET.

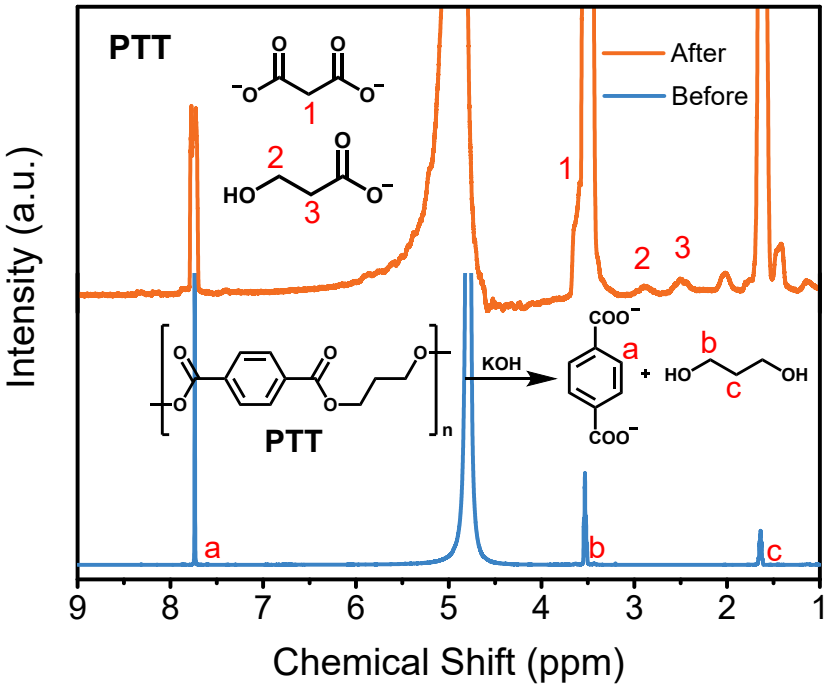

Fig. S19 ^{1}H NMR spectra of products before and after photoreforming of PTT.

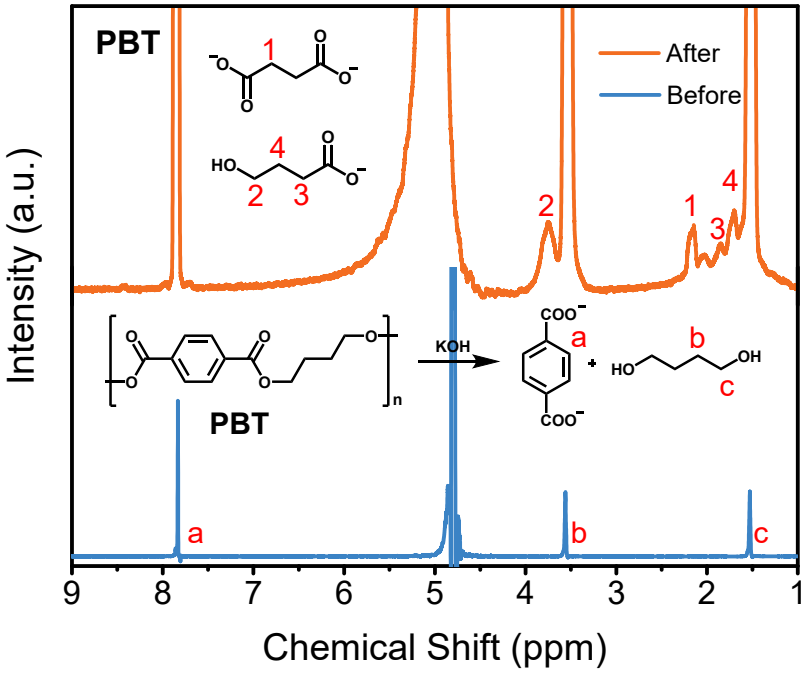

Fig. S20 ^{1}H NMR spectra of products before and after photoreforming of PBT.

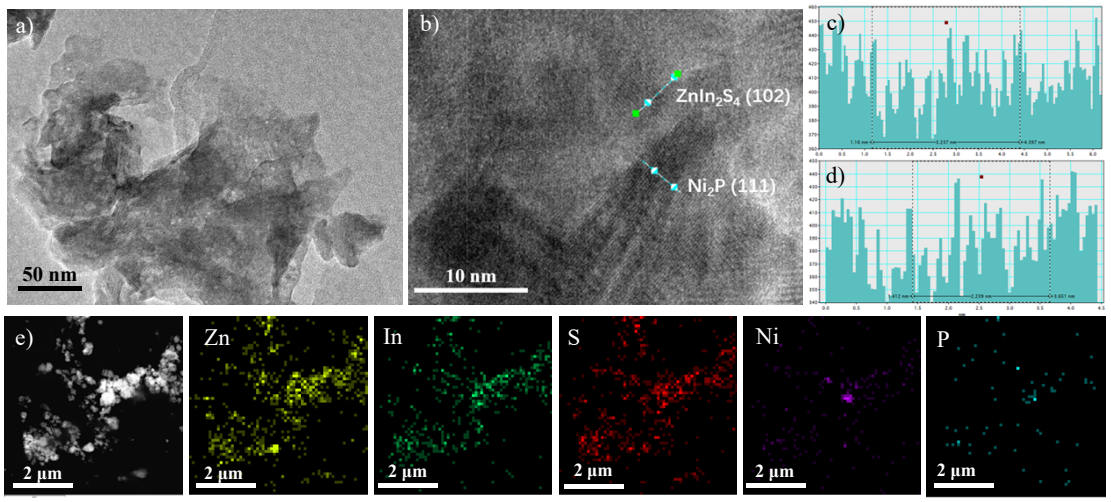

Fig. S21 The morphology of the samples after a long-term photoreforming.

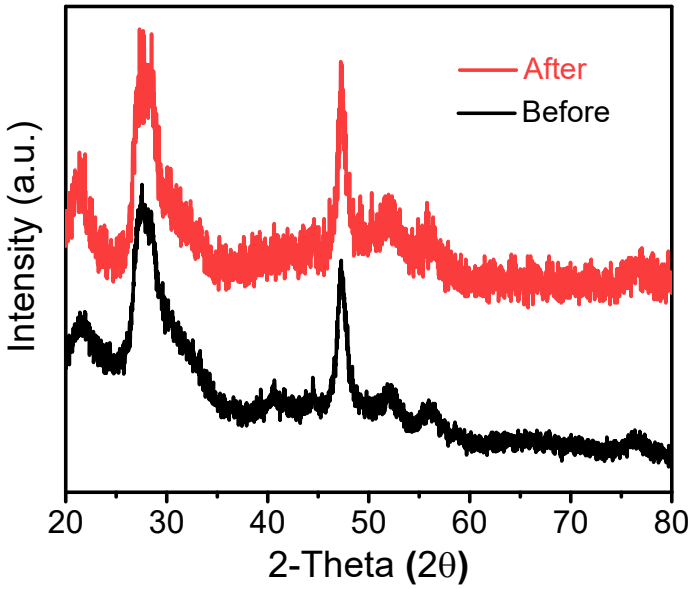

Fig. S22 XRD of $Ni_2P/ZnIn_2S_4$ before and after photocatalytic reaction.

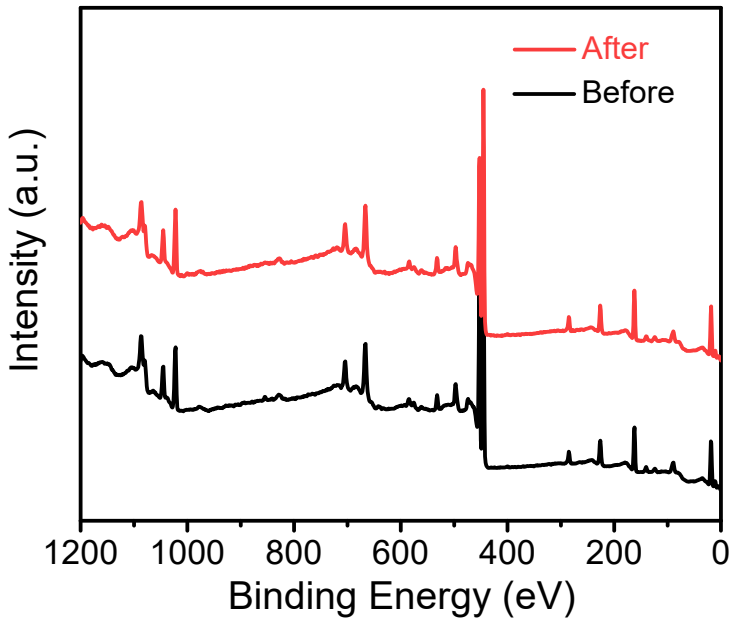

Fig. S23 XPS of $Ni_2P/ZnIn_2S_4$ before and after photocatalytic reaction.

Table S1. EDX results of elements in the 7.5-$Ni_2P/ZnIn_2S_4$ composites.

Element	Weight%	Atomic%
P K	1.13	2.27
S K	21.18	41.05
Ni K	7.87	8.33
Zn K	25.80	24.53
In L	44.02	23.82
Totals	100.00	

Table S2. ICP results of elements in the $Ni_2P/ZnIn_2S_4$ composites.

	1-$Ni_2P/ZnIn_2S_4$	3-$Ni_2P/ZnIn_2S_4$	5-$Ni_2P/ZnIn_2S_4$
Zn (wt%)	13.471	13.818	13.985
In (wt%)	55.743	53.405	51.850
Ni (wt%)	0.800	1.803	3.591